JSTEM

Single molecular investigation of the interactions between cationic short peptides and DNA

Xuetong He, Weiyu Wu, Lingxuan Kong, Guangcan Yang* and Yanwei Wang*

College of Mathmatics and Physics, Wenzhou University, China
wangyw@wzu.edu.cn ; yanggc@wzu.edu.cn

Abstract: Intracellular liquid-liquid phase separation (LLPS) plays several crucial roles in cellular biology, including the regulation of biochemical reactions and gene expression. These processes can involve interactions between proteins (and/or peptides) and specific DNA sequences. In this study, we explored the interaction between DNA and two types of cationic peptides, polyarginine and polylysine, using magnetic tweezers (MT) and atomic force microscopy (AFM). We found that polyarginine is more effective at inducing DNA compaction than polylysine at the same concentration. We attribute this effect to polyarginine's greater efficiency in neutralizing DNA's surface charge, which was confirmed through electrophoretic mobility measurements using dynamic light scattering (DLS). Our study compares the effects of polyarginine and polylysine on DNA, revealing that polyarginine, despite having the same charge, has a superior ability to neutralize DNA's surface charge at equivalent concentrations.

Keywords: cationic short peptides, DNA, LLPS

1. Introduction

Liquid-liquid separation may react between peptides and DNA or RNA. One study showed that poly R droplets are over 100× more viscous than poly K[1]. It perhaps causes Poly R or Poly K to produce different results when interacting with DNA or RNA. Lysine plays several roles in humans, most importantly proteinogenesis, the cross-linking of collagen polypeptides, the uptake of essential mineral nutrients, and the production of carnitine, which is crucial in fatty acid metabolism. Lysine is also often involved in histone modifications and thus, impacts the epigenome. Arginine plays an essential role in cell division, wound healing, removing ammonia from the body, immune function, and the release of hormones. It is a precursor for the synthesis of nitric oxide (NO), making it essential in regulating blood pressure[2].

The molecular and functional differences between arginine and lysine residues make them an ideal model system for extracting fundamental principles bridging sequence, material, and operational levels[3]. In addition to unique roles in liquid phase separation discussed above, arginine specificity over lysine residues appear in other functional parts, including membrane interactions, cell entry of antimicrobial peptides, and regulation of voltage-gated ion channels. Arginines are also more efficient at RNA binding65[4]. Recent work suggests that proline–arginine dipeptide repeats interact more strongly with RNA oligonucleotides than proline–lysine repeats due in part to enhanced pi–pi interactions[5].

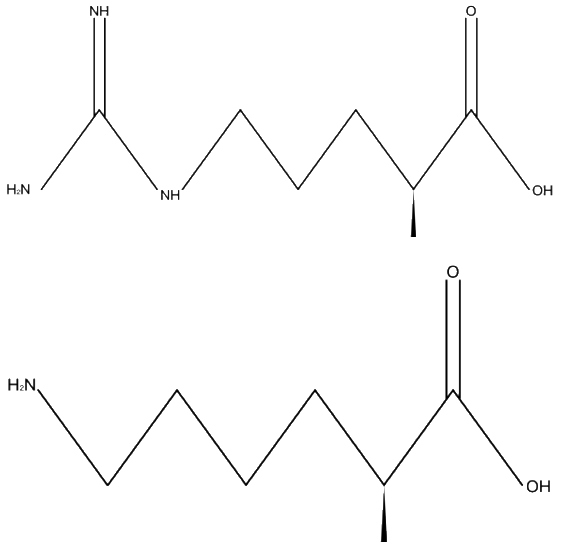

Figure 1. Molecular structure of polyarginine and polylysine. Arginine has two more residues than lysine. Figure (a) shows arginine; (b) shows lysine.

Previous studies have shown that arginine has a strong effect on the sustained length of DNA when arginine and lysine interact with DNA separately. However, the former used small-angle X-ray experiments to determine the interaction of DNA with arginine or lysine at various energies[6]. Experimental results show that when arginine cell division, wound healing, removing ammonia from the body, immune function, and the release of hormones. It is a precursor for the synthesis of nitric oxide (NO), making it essential in regulating blood pressure[7].

The molecular and functional differences between arginine and lysine residues make them an ideal model system for extracting fundamental principles bridging sequence, material, and operational levels [3]. In addition to unique roles in liquid phase separation discussed above, arginine specificity over lysine residues appear in other functional parts, including membrane interactions, cell entry of antimicrobial peptides, and regulation of voltage-gated ion channels[8]. Arginines are also more efficient at RNA binding65. Recent work suggests that proline–arginine dipeptide repeats interact interacts with DNA under the same circumstances, the sustained length of DNA increases.

DNA condensation is an essential process for its high-density packing in biological systems, particularly in viruses and sperm cells, and has found applications (either by design or luck) in artificial gene delivery[9]. In this process, DNA undergoes a dramatic condensation to a compact structure in the presence of various agents, such as multivalent cations[10],alcohol, essential proteins, neutral crowding polymers, cationic liposomes, and anti-cancer drugs[11]. This phenomenon has drawn considerable attention and induced related studies in different past decades, especially by the recently developed single-molecule techniques[12].

The single-molecule approaches allow us to study the behavior of biological macromolecules under applied tensions; the mechanical properties of these molecules help us understand how they function in the cell[13]. They can usually be classified into two major categories: mechanical force transducers and external field manipulators. In the mechanical force transducers—the AFM, microneedles, and optical fibers—forces are applied or sensed through bendable beams. In the external field manipulators— optical tweezers (OT), magnetic tweezers (MT), and flow fields— the molecule is acted upon from a distance, by application of external fields (photonic, magnetic, or hydrodynamic) either to the molecule itself or to an appropriate handle to which the molecule is attached[14]. Among them, single-molecule magnetic tweezers are versatile and inexpensive instruments. This technique allows the application of a constant pulling force on a single DNA molecule while measuring its elongation in real-time. For instance, Fu et al. studied the compaction dynamics of a single DNA molecule invoked by hexamine cobalt chloride. The observations suggested that the

folding/unfolding is a reversible transition between two metastable structural states. However, Besteman et al. investigated DNA condensation by cobalt burial and showed that condensation under tension is an activated process that is irreversible on experimental time scales.

2. Method and material

We use Single molecule operation include Magic Tweezers (MT), Dynamic Light Scattering (DLS) and Aton Force Microscope (AFM). Reagent Preparation. Double-strand λ-phage DNA (48502 bp) for MT and AFM measurements was purchased from New England Biolabs Co. and did not go through purification before use. The stock solution of DNA was 1 × TE buffer (10 mM Tris-HCl and 1 mM EDTA, pH = 8.0), and the DNA concentration was 500 ng/μL. Poly R, Poly K ,Poly RH and Poly KH was purchased from GL Biochem (Shanghai) Ltd. and did not go through purification before use.

2.1 MT Measurement

This is a very mature single-molecule manipulation technique.A home-built transverse MT setup built on an inverted microscope (Nikon TE2000U) was used to study the DNA–peptides binding dynamics. A sandwich-like flow cell was constructed to anchor single DNA molecules[15]. In the magnetic tweezers experiment, through a fixed sample cell, a lower concentration of peptide is introduced into the sample cell, and the concentration of the injected peptide is gradually increased until the DNA undergoes an obvious aggregation reaction. At the same time, record the concentration of the peptide passing through the reaction and compare it with another peptide with the same number of amino acids. The side wall of the chamber was first coated with anti-digoxigenin to link the dig-end of the modified DNA. The DNA– bead constructs prepared as described in the 'Material' section were then allowed to flow into the cell and incubated for about 15 min to form sidewall-DNA-bead structures. It can measures condensing force of DNA under different peptides like Poly R3/K3.

2.2 Magic tweezers force calculate

The force exerted by the tweezers cannot be determined from first principles if only because magnetization varies from one bead to another. Instead, the instrument relies on quantification of Brownian motion of the bead[16]. To this end, the thermal motion of the bead is recorded at several positions of the magnets, quantified to derive the forces acting on the bead, and the measured forces are then used to construct an empirical interpolation function. Different interpolation functions have been employed for the task including high power polynomials and the exponential function $F = F_{max} \exp (AZ_{mag}+BZ_{mag})^2$. In this analysis, the bead must be suspended in solution since its interactions with the surface restrict its motion and leads to abnormal readings[17].

In principle, the force can be calculated from the magnitude of the horizontal bead fluctuations, <δy2>. According to the Equipartition Theorem, $\alpha y<\delta y2>=kT$, where αy is the horizontal stiffness of the trap, T is the temperature and k is the Boltzmann constant . For a bead tethered to the surface via a single linkage, the stiffness is proportional to the applied force, $\alpha y = F/l$, where l is the length of the tether, leading to the following relationship:

$$F = \frac{kTl}{< \delta y^2 >} \quad (1)$$

Thus, the force can be readily computed once the length of the tether and the variance of fluctuations are known. In practice, however, the utility of Equation (1) is limited due to external vibrations in the instrument, which must be filtered out from the recorded Brownian motion. The most robust way to achieve it is by fitting the fluctuations in the frequency domain[15].

A detailed description of such analysis and associated problems is presented in Berg-Sorensen and Flyvbjerg. The approach is based on solving the underlying Langevin equation in the frequency domain. Assuming a harmonic force field, the power spectrum of the bead motion is found to be the Lorentzian:

$$S(f) = \frac{kT}{\pi^2 \zeta (f^2 + f_0^2)} \quad (2)$$

where S(f) is the power spectrum of the bead motion, ζ is the friction coefficient for the bead, and f0 = αy/2πζ is the cut off frequency of the oscillator. For a spherical particle with the radius r in a liquid with the viscosity η, ζ = 6πηr. Regardless to the shape of the bead, the friction coefficient is related to its diffusion coefficient, D, via the Einstein equation, D=kT/ζ. Integration of Equation (2) over the entire range of frequencies (from zero to infinity) yields Equation (1)[18].

2.3 AFM Measurement

To observed peptides effect DNA morphologies mediated by divalent counterions directly, we used AFM to observe DNA conformational changes under the different peptides. The DNA morphologies imaging was performed in air with a multimode AFM with nanoscope controller (JPK NanoWizard3 Nano Science) in the AC mode. Experiments were performed by 1 mM Tris. The fial concentration of DNA was 1 ng/μL.The mica is cut into 1cm x 1cm square sheets and dissociated 3 to 5 times to obtain the mica sheet for imaging substrate. The DNA to peptide ratio of 200:0.4 was added to obtain a 1ng/ul concentration of DNA solution for AFM imaging. Such as taking 0.08ng/ul poly K4 200ul, adding 0.4ul DNA, mixing, and shaking well for 30 minutes. Then, take an appropriate amount of mixed solution, drop it on the treated mica for deposition for 3 minutes, wash it with ultra-purify water eight times, and put it into the drying oven for 8 hours for imaging.

2.4 DLS Measurement

The electrophoresis-mobility measurements were carried out by using a dynamic light scattering device of Malvern Zeta sizer Nano ZS90 (Malvern Instruments Ltd., Worcestershire, UK) equipped with the patented M3-PALS technique. The laser source is a He-Ne gas laser (1 = 633 nm) and the light scattering is collected by an avalanche photodiode mounted on the goniometer arm to the direction of the incident radiation. The DNA samples were diluted to a concentration of 1 ng /μL in a Tris solution; then, different concentrations of Poly R or Poly K were added. All measurements were carried out after 5 min incubation at room temperature. During the measurement, 1 mL of DNA solution was used, and the sample cell was kept at 25 °C temperature.

3. Result and discussion

3.1 Condensation of DNA measurement

We examined the sensitivity of DNA condensation to multivalent cation concentration by measuring the stretching response of single bacteriophage -DNA molecules at different multivalent cationic short peptidesconcentrations. We first find a single λ-DNA molecule tethered in PBS. Then, we flow different concentration of Poly R or Poly K at different member of amino acid to the sample cell. We flowed the same concentration of Poly K3 or Poly R3 at 100 ng/μl to the cuvette. As shown in Figure 2, DNA coalescence is more pronounced in the presence of polyarginine in solutions of the same concentration.

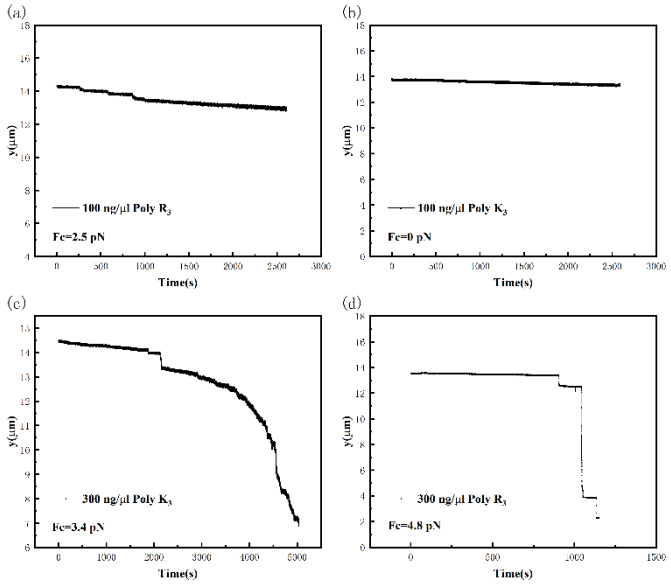

Figure 2. MT force spectrum images of polyarginine and poly lysine with the same amount of positive charge. (a). 100 ng/ul Poly R3; (b). 100ng/ul Poly K3. (c). 300ng/ul Poly R3 (d). 300 ng/ul Poly K3.

Figure 2 shows the MT measurements of the cationic short peptides polyarginine and polylysine with three charges. The results of MT measurements at a Poly R3 concentration of 100 ng/ul has shown in Fig.(2a). After the previously mentioned calculation method, DNA cohesion Fc is 2.5 pN. Similarly, Fig.(2b), Fig.(2c), and Fig.(2d) cohesion Fc are 0 pN, 3.4pN, and 3.8pN in that order. For polyarginine or polylysine, the DNA cohesion increases with elevated concentrations. Interestingly, at 100 ng/ul concentration, polyarginine caused some cohesive effect on DNA, but polylysine did not respond. The DNA cohesion has been calculated in several experiments, and the final cohesion has been calculated and calculated as shown in Table 1.

Poly-peptides / Concentration	Poly R3	Poly K3
100	2.5pN±0.25	0
300	4.8pN±0.31	3.4pN±0.18
500		

Table 1. Cohesion statistics for DNA and Poly R3 or Poly K3 mixtures

To further verify our conclusion, we replaced the peptide with three amino acids with a peptide with four amino acids to perform the above experiment. The results are shown in Fig 3.

Likewise, this trend also occurs with Poly R4 compared to Poly K4. DNA cohesion increases with the concentration of poly R4 or poly K4. Fig. 3a and 3c or 3b and 3d show that DNA cohesion increases with the increase of Poly R4 or Poly K4 concentration. In addition, Poly R4 and Poly K4 at the same concentration also have specific differences. After analysis and calculation, the DNA cohesion of Poly R4 was 2.1pN, and Poly K4 was 1.1pN when the concentration was 50ng/ul. When the concentration was increased to 100ng/ul (Fig.3c and Fig.3d), the results were the same as in the previous experiment. Polyarginine is more efficient in making DNA cohesion. As mentioned earlier, comparing the ability of polyarginine and polylysine to coalesce DNA, polyarginine is significantly more efficient.

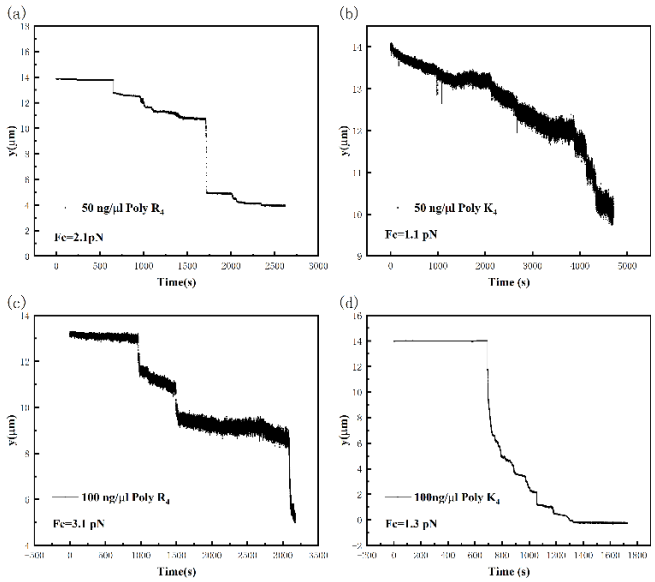

Figure 3. replaced with images of MT force spectra of polyarginine and polyarginine with four cations. Fig.(a).50 ng/ul Poly R4; Fig.(b) 50 ng/ul Poly K4; Fig. (c) 100ng/ul Poly R4; Fig.(d) 100 ng/ul Poly K4

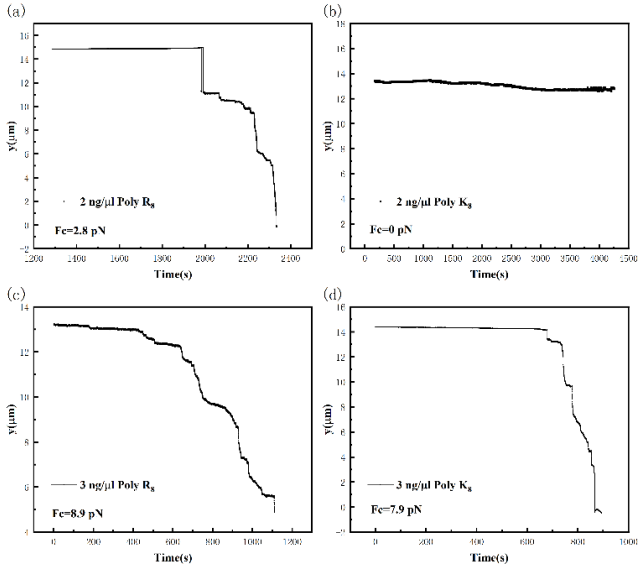

Figure 4. MT force spectra of polyarginine and polylysine with eight charges interacting with DNA. Figure (a) 2ng/ul Poly R8; Fig.(b) 2ng/ul poly K8 ; Fig.(c) 3ng/ul Poly R8 ; Fig.(d) 3ng/ul Poly K8.

The same thing happens with poly octa-arginine and poly octa-lysine, as shown in Figure 4. Since the number of positive charges of polyoctagarginine or polyoctaglysine is eight, DNA cohesion changes very rapidly with the concentration of polypeptides. MT curves of polyoctagarginine and polyoctaglysine were obtained according to the previous method. As shown in Fig. 4a and Fig. 4c or Fig. 4b and 4d, when we increased the concentration of Poly R8 or Poly K8, DNA cohesion also increased. Polyarginine is still more effective for DNA condensation when concentrations are consistent (fig.4c and fig.4d). Comparing Fig. 4a and Fig. 4b, polyarginine causes significant cohesion of DNA but polylysine can not.

Summarizing this MT data, it becomes evident that polyarginine has a better effect on DNA cohesion with the same charge.

3.2 Electrophoretic Mobility of DNA

To verify our conclusions from various aspects, we used dynamic light scattering experiments to measure the changes in the zeta potential of DNA under the influence of peptides. We measured the electrophoretic mobility of DNA in the mixture solution with different concentrations of Poly R and Poly K by dynamic light scattering technique. The result is shown in Figure 4.

Poly R3 measurements were found to be higher than Poly K3 at a concentration of 300ng/ul. Therefore, Poly R3 is more likely to reverse the charge of DNA than Poly K3.21. For example, when the concentration of Poly R3 is 300 ng/ul, μ is about 0.18 (in units of 10−4 cm2V−1s−1, the same unit is used for mobility in the following and will not be indicated for clarity) but Poly K3, μ is about -0.2. According to the above experimental data, when Poly R3 and Poly K3 are at the same concentration, μ of Poly R3 is always greater than Poly K3. This also means comparing polyarginine and polylysine. Polyarginine has a more efficient effect on DNA surface charge.

Similarly, to further verify our conclusion, we replaced poly tri-arginine and poly tri-lysine with poly tetra-arginine and poly tetra-lysine. Following the same experimental procedure has shown in Figure 6, the upward trend of electrophoretic mobility of both is consistent.

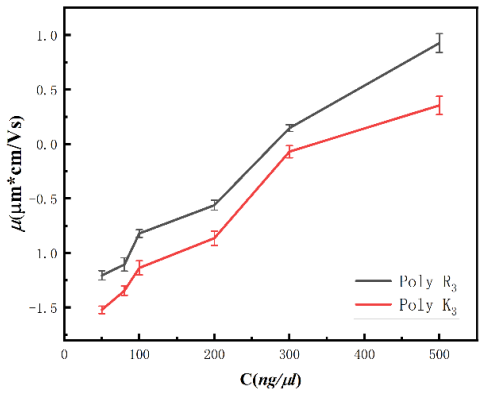

Figure 5. Polyarginine and polylysine with DNA, respectively, and DNA table charge changes. The curve of Poly R3 consistently stays above the curve of Poly K3. The zeta potential is higher for Poly R3 when comparing Poly R3 and Poly K3 at arbitrary concentrations.

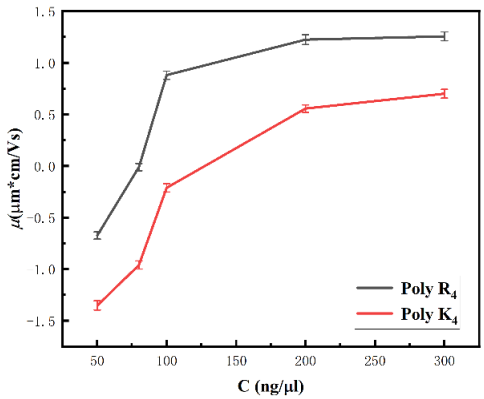

Figure 6. Polyarginine and polylysine with DNA, respectively, and DNA table charge changes. The curve of Poly R4 consistently stays above the curve of Poly K4. The zeta potential is higher for Poly R4 when comparing Poly R4 and Poly K4 at arbitrary concentrations.

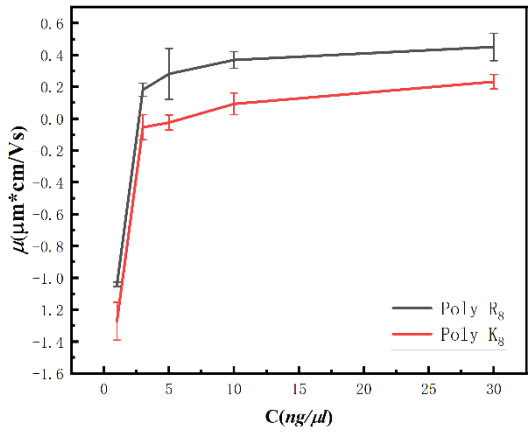

Figure 7. Polyarginine and polylysine with DNA, respectively, and DNA table charge changes. The curve of Poly R4 consistently stays above the curve of Poly K4. The zeta potential is higher for Poly R4 when comparing Poly R4 and Poly K4 at arbitrary concentrations. The zeta potential of Poly R8 was already greater than zero at a concentration of 3 ng/ul, while the zeta potential of Poly K3 only approached zero at a concentration of 3 ng/ul.

The zeta potential of Poly R4 was very close to zero at a concentration of 80 ng/ul, while the zeta potential of Poly K4 was close to zero at a concentration of 100 ng/ul. It can still be seen that the DNA surface charge is neutralized more rapidly in the presence of poly tetra arginine at the same concentration. In other words, poly tetra arginine is more likely to cause charge reversal in DNA. The same thing happens when we change to poly octa-arginine and poly octa-lysine has shown in figure 7. Since both Poly R8 and Poly K8 have eight positive charges, they have a powerful effect on DNA. This also results in low concentrations that cause the DNA surface charge to be neutralized, meaning that the zeta potential increases significantly. The change in zeta potential is very rapid even when the concentration is raised by 1 ng/ul each time.

From the data of the three DLS experiments, we can further confirm our conclusion that the ability to make DNA cohesion with arginine is more efficient.

3.3 Atomic force microscopy measurements

To obtain the information on the structure of the DNA/Poly R3 or Poly K3 complex, we observed DNA complexes using atomic force microscopy at different concentrations of peptides [19].

Using the method described in the materials and methods

section, Poly R3 and DNA mixture at a concentration of 50 ng/ul was observed and the DNA coalesced into clumps (Fig.8a). When the concentration of Poly R3 is increased to 300 ng/ul, we can see the toroid morphologies on the mica surface in Fig. 8c. Similarly, Poly K3 was chosen for 50 ng/ul and 300 ng/ul. As shown in Fig.8b, at a poly K3 concentration of 50ng/ul, the DNA morphology resembles free and loose wool. When the concentration is increased to 300ng/ul (Fig.8d), the DNA becomes more compact but not yet coalesced into small balls.

In both Poly R and Poly K, the degree of DNA cohesion became stronger with the increasing concentration of the polypeptide. Comparing A Poly R and Poly K, we found that polyarginine was more effective on DNA cohesion with the same charge.

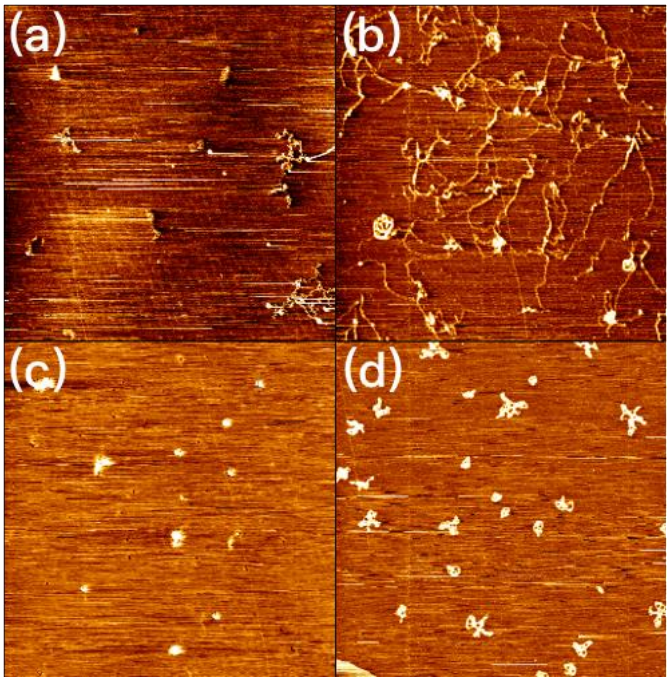

Figure 8. AFM images of the effect of Poly R3 and Poly K3 on DNA confirmation at the same concentration. (a) DNA coalesced into small clusters in the presence of R3 at a concentration of 50 ng/μl.(b) At a concentration of 50 ng/μl of K3, (c) At 300 ng/μl of R3, (d) K3 at 300 ng/μl, DNA.

4. Discussion

The underlying reason for the weaker attraction of lysine peptides compared to arginine peptides is not clear. It may not be due to an intrinsic difference in the interhelical attraction of charged amine and guanidine groups[20].

Combining the results of this study with those of available previous studies, we conjecture that it may be that the larger spacing with lysine peptides is caused by both a weaker attraction and a stronger short-range repulsion relative to that of the arginine peptides. A previously proposed model for binding polyarginine and protamine to DNA provides a convenient framework for understanding the differences between the ability of lysine and arginine peptides to assemble DNA[21]. Not only that, but in terms of hydrophobicity, arginine is more hydrophobic than lysine, which makes it more likely to repel water molecules in the vicinity of DNA, making it easier for DNA to coalesce into "blobs"[22].

In addition to the two possible reasons mentioned above, another reason could be One proposed arrangement of DNA and cation charges that can result in favorable correlations is that cations bind in DNA grooves[23]. Adjacent helices can position themselves for a favorable interaction of the positively charged groove of one helix with the negatively charged backbone of another. Because the major groove of B-form DNA is significantly wider than the minor groove[24], the positive−negative charge separation and, hence, the attractive force could be greater for cations that bind in the major groove than for those that bind in the minor groove. The difference between the DNA−DNA forces with lysine and arginine peptides most likely is the result of a difference in details in the binding mode[25].

Conclusion

In this study, we separately validate our findings from MT, DLS, and AFM three directions to verify our obtained conclusions. In the MT experiment, comparing polylysine and polyarginine, we can see that either poly tri arginine,

polytetraarginine or polyoctaarginine results in greater DNA cohesion. In the DLS experiments, similar conclusions were obtained, comparing polyarginine and polylysine, polyarginine always neutralizes the DNA surface charge faster, i.e. the zeta potential tends to 0 faster. In the AFM experiments, we observed more visually that polyarginine makes DNA cohesive more easily, even into small spheres.

The difference in the ability of arginine and lysine peptides to compact DNA is quite substantial. The large difference in forces between structurally similar arginine and lysine peptides emphasizes the importance of the conformation of the bound cation in creating interhelical correlations. The model of Hud et al[26].for binding of arginine to DNA extended to lysine is consistent with our observations.

Acknowledgements

This work is supported by the National Natural Science Foundation of China (12074289, 11574232) and the Natural Science Foundation of Zhejiang Province(LY23A40002). Wenzhou science and Technology Prpject（L20240004）.The 14th Five-Year Plan Teaching Reform Project of Higher Education in Zhejiang Province (JG20220509) and the Graduate Teaching Reform Project (2023-016);Industry-University-Research Project of Ministry of Education(202101003050,202101044006).

Notes and references

1. Fisher, R.S. and S. Elbaum-Garfinkle, Tunable multiphase dynamics of arginine and lysine liquid condensates. Nature communications, 2020. 11(1): p. 4628.
2. Shin, Y. and C.P. Brangwynne, Liquid phase condensation in cell physiology and disease. Science, 2017. 357(6357): p. eaaf4382.
3. Paloni, M., G. Bussi, and A. Barducci, Arginine multivalency stabilizes protein/RNA condensates. Protein Science, 2021. 30(7): p. 1418-1426.
4. Suzuki, H., et al., The proline–arginine repeat protein linked to C9-ALS/FTD causes neuronal toxicity by inhibiting the DEAD-box RNA helicase-mediated ribosome biogenesis. Cell death & disease, 2018. 9(10): p. 975.
5. Boeynaems, S., et al., Spontaneous driving forces give rise to protein− RNA condensates with coexisting phases and complex material properties. Proceedings of the National Academy of Sciences, 2019. 116(16): p. 7889-7898.
6. Yoo, J., D. Winogradoff, and A. Aksimentiev, Molecular dynamics simulations of DNA–DNA and DNA–protein interactions. Current Opinion in Structural Biology, 2020. 64: p. 88-96.
7. Appleton, J., Arginine: clinical potential of a semi-essential amino acid.(Arginine). Alternative medicine review, 2002. 7(6): p. 512-523.
8. Raghuraman, H. and A. Chattopadhyay, Melittin: a membrane-active peptide with diverse functions. Bioscience reports, 2007. 27(4-5): p. 189-223.
9. Wang, Y., et al., Ethanol induces condensation of single DNA molecules. Soft Matter, 2011. 7(9): p. 4425-4434.
10. Baumann, C.G., et al., Ionic effects on the elasticity of single DNA molecules. Proceedings of the National Academy of Sciences, 1997. 94(12): p. 6185-6190.
11. Bloomfield, V.A., DNA condensation. Current opinion in structural biology, 1996. 6(3): p. 334-341.
12. Size, D., TOROIDAL DNA CONDENSATES: Unraveling the. Annu. Rev. Biophys. Biomol. Struct, 2005. 34: p. 295-318.
13. Zlatanova, J. and S.H. Leuba, Magnetic tweezers: a sensitive tool to study DNA and chromatin at the single-molecule level. Biochemistry and cell biology, 2003. 81(3): p. 151-159.
14. Sarkar, R. and V.V. Rybenkov, A guide to magnetic tweezers and their applications. Frontiers in Physics, 2016. 4: p. 48.

15. Liu, Y.-F. and S.-Y. Ran, Divalent metal ions and intermolecular interactions facilitate DNA network formation. Colloids and Surfaces B: Biointerfaces, 2020. 194: p. 111117.
16. Lipfert, J., et al., Magnetic torque tweezers: measuring torsional stiffness in DNA and RecA-DNA filaments. Nature methods, 2010. 7(12): p. 977-980.
17. Wang, Y., et al., DNA condensations on mica surfaces induced collaboratively by alcohol and hexammine cobalt. Colloids and Surfaces B: Biointerfaces, 2011. 83(1): p. 61-68.
18. Burnham, D.R., et al., Skewed brownian fluctuations in single-molecule magnetic tweezers. PloS one, 2014. 9(9): p. e108271.
19. Wang, Y., et al., Single molecular demonstration of modulating charge inversion of DNA. Scientific Reports, 2016. 6(1): p. 38628.
20. Li, L., I. Vorobyov, and T.W. Allen, The different interactions of lysine and arginine side chains with lipid membranes. The journal of physical chemistry B, 2013. 117(40): p. 11906-11920.
21. Plank, C., et al., Branched cationic peptides for gene delivery:: Role of type and number of cationic residues in formation and in vitro activity of DNA polyplexes (vol 10, pg 322, 1999). Human Gene Therapy, 1999. 10(13): p. 2272-2272.
22. Bergeron-Sandoval, L.-P., N. Safaee, and S.W. Michnick, Mechanisms and consequences of macromolecular phase separation. Cell, 2016. 165(5): p. 1067-1079.
23. Korolev, N., et al., A molecular dynamics simulation study of oriented DNA with polyamine and sodium counterions: diffusion and averaged binding of water and cations. Nucleic acids research, 2003. 31(20): p. 5971-5981.
24. Drew, H.R. and R.E. Dickerson, Structure of a B-DNA dodecamer. Journal of Molecular Biology, 1981. 151(3): p. 535-556.
25. Kornyshev, A. and S. Leikin, Electrostatic zipper motif for DNA aggregation. Physical review letters, 1999. 82(20): p. 4138.
26. Hud, N.V., F.P. Milanovich, and R. Balhorn, Evidence of novel secondary structure in DNA-bound protamine is revealed by Raman spectroscopy. Biochemistry, 1994. 33(24): p. 7528-7535.